

## Research Article

# Photodetector Based on Titanium Oxide Nanoparticles Produced via Pulsed Laser Ablation

**Ban A. Bader,<sup>1</sup> Iman H. Hadi,<sup>2</sup> Muna Y. Slewa,<sup>1</sup> Khawla S Khashan ,<sup>2</sup> and Farah A. Abdulameer<sup>3</sup>**

<sup>1</sup>Department of Physics, College of Education, University of Al-Hamdaniya, Al-Hamdaniya, Nineveh, Iraq

<sup>2</sup>Applied Sciences Department, University of Technology, Baghdad, Iraq

<sup>3</sup>College of Health and Medical Techniques, Gilgamesh Ahliya University, Baghdad, Iraq

Correspondence should be addressed to Khawla S Khashan; 100082@uotechnology.edu.iq

Received 13 September 2022; Revised 8 October 2022; Accepted 20 October 2022; Published 28 October 2022

Academic Editor: Ashwini Kumar

Copyright © 2022 Ban A. Bader et al. This is an open access article distributed under the Creative Commons Attribution License, which permits unrestricted use, distribution, and reproduction in any medium, provided the original work is properly cited.

TiO<sub>2</sub> nanoparticles (NPs) were produced via utilized nanosecond laser ablation of titanium in water. The description of these NPs was employed utilizing XRD, SEM, and UV-VIS. Then, optoelectronic properties were investigated via a drop-casting of TiO<sub>2</sub> NPs on the Si wafer substrate. XRD results show the formation of anatase TiO<sub>2</sub>. The SEM exhibits a spherical shape with sizing changing from 5 nm to 50 nm. The bandgap was 3.6 eV which was determined from the Tauc chart. The IV characteristic of the TiO<sub>2</sub>NPs/Si heterojunction showed good rectifying behaviour, with a maximum responsivity of about 0.7 A/W at 310 nm.

## 1. Introduction

Metal oxide nanostructure material is a very interesting nanomaterial owing to its unique electric, magnetic, optical, and chemical characterization [1]. These characterizations make them suitable to be applied in different application areas like solar cells, photodetectors, catalysts, antimicrobial sensors, and batteries [2–6]. TiO<sub>2</sub> nanostructure material is one of the excellent metal oxide semiconductor materials owing to its important features like high transparency, high refractive index, good chemical stability, relative hardness, and wide gap. These material oxides exist in three diverse structure systems: rutile (tetragonal), anatase (trigonal), and brookite (orthorhombic) [7–12]. Many techniques were applied to prepare TiO<sub>2</sub> nanoparticles like sol-gel, chemical vapor deposition, sputtering, and hydrothermal method [13–18]. Nanosecond pulsed laser ablation method in the fluid environmental process is a very appropriate procedure to produce TiO<sub>2</sub> NPs with different sizes, shapes, and forms depending on the laser ablation parameters like wavelength, fluence, number of laser pulses, and liquid medium. Recently, it has provided a good, simple, and low-cost procedure for the production of size-controlled nanoparticles in

solution with a high purity of nanoparticles [19–24]. In this process, irradiation of a target, which is immersed in a liquid with a pulse, starts the foundation of plasma and removal of material. These plasmas have species like ions, atoms, and clusters. The species in the plume collide and react with molecules of the surrounding medium, generating new compounds including atoms from both the target and the solution. Moreover, due to high-density conditions, this method provides manufacturing of unique materials which are inaccessible using traditional methods [8, 9, 12]. Therefore, many researchers have utilized the production of nanoparticles such as metal oxide, nitride, carbon, metal, and metal carbide via laser ablation in liquid [25–29]. In this research, we prepare TiO<sub>2</sub> NPs using pulsed (ns) laser ablation in solution and investigate the optoelectronic features.

## 2. Materials and Method

The process of laser ablation was used to produce TiO<sub>2</sub>NPs in deionized water. TiO<sub>2</sub>NPs were produced by employing a 1064 nm Q-switched pulsed Nd: YAG laser (200 mJ, 7 ns) to ablate titanium plate immersed in (2 ml) deionized water (DIW), operated with 200 mJ and 150 pulses. A structure of

TiO<sub>2</sub> NPs was examined by X-ray diffraction (600-Shimadzu; CuK $\alpha$  = 1.54060 Å), the topography and nanosized of TiO<sub>2</sub>NPs were determined via SEM from TESCAN, and the absorption was assessed via Shimadzu 1800 UV-VIS spectrophotometer. To measure the optoelectronic properties, the TiO<sub>2</sub> NPs were deposited on a silicon substrate by the drop-casting process. A dark current-voltage characterization was carried out using a Tektronix CDM 250 and power supply. The responsivity of the TiO<sub>2</sub> NPs/Si heterojunction photodetector was evaluated in a spectral range (200–500) nm employing a calibrated monochromator.

### 3. Results and Discussion

Figure 1 indicates XRD pattern of TiO<sub>2</sub>NPs produced in DIW by laser ablation at 200 mJ for 150 laser pulses. The spectrum exhibits peaks at  $2\theta = 25.2^\circ$ ,  $36.4^\circ$ , and  $38.9^\circ$  which are assigned to (101), (103), and (112) phases that are matched to the crystal planes of anatase TiO<sub>2</sub> (JCPDS 21-1272) [7]. The size of the TiO<sub>2</sub> nanostructure ( $D$ ) was determined by the Debye-Scherrer equation [7]:  $D = 0.94\lambda/\beta \cos \theta$ , where  $\lambda$  is the X-ray wavelength,  $\theta$  is the angle of Bragg's diffraction, and  $\beta$  is full width at half maximum. This data is shown in Table 1.

Figure 2 exhibits an SEM image of TiO<sub>2</sub>NPs prepared via 200 mJ and 150 pulses. The image shows that the particles have a spherical-like shape and size changes from 5 nm to 50 nm. Also, there is an individual particle that can be seen with high aggregations owing to the electrostatic attractive force through nanoparticles. As a result of the interaction between laser radiation and the submerged titanium target, a very thin layer of Ti metal is heated to its melting point. The solvent layer near to the Ti metal warms up to a temperature which is substantially higher than the liquid's boiling temperature at atmospheric pressure as a result of the transfer of heat from the metal to the surrounding medium. The outcome is the formation of bubbles. TiO<sub>2</sub>NPs is created as an effect of the reaction among the molten metal and the oxygen in the evaporated solvent. This technique was used to create nanoparticles of various shapes and sizes. For example, Fadhil et al. [6] prepared CuO NPs with a size change from 10 nm to 100 nm; Khashan and Abbas [19] used the same technique to create spherical-shaped Indium nitride (InN) nanoparticles with particle sizes in the range of 2–20 nm; as well as Khashan and Mahdi [21] to create ZnMgO nanocomposites with a flower-like hierarchical structure and a full array of about 2  $\mu$ m. While, Hameed et al. [24] generated carbon nanoparticles separated long multi-wall carbon nanotubes (MWCNT) with hollow core in different dimensions, larger in diameter (66–75) nm and other sizing about (25–30) nm. Khashan et al. [29] produced silicon carbide nanoparticles with spherical shape and average size ranging from 25 nm to 55 nm.

Figure 3 exhibits the relationship between  $(ah\nu)^2$  and  $(h\nu)$  of TiO<sub>2</sub> nanoparticles, while the insert in the figure demonstrates the change of absorption per a wavelength. The bandgap was determined from extrapolating the linear part in Figure 3, and it was found to be 3.6 eV. The larger energy gap for TiO<sub>2</sub>NPs compared to its bulk value (3.2 eV)

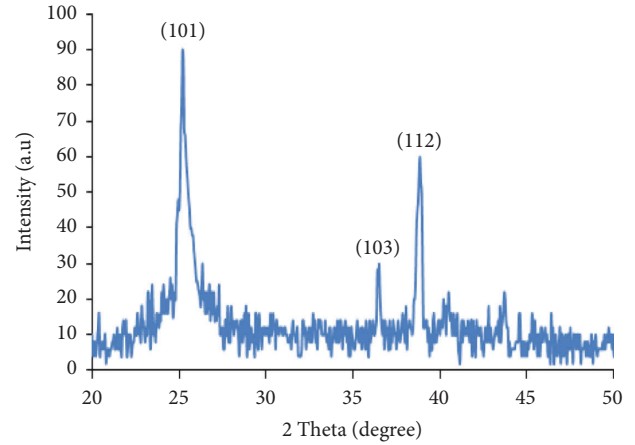


FIGURE 1: XRD pattern of TiO<sub>2</sub>NPs.

may provide confirmation for the quantum size effects. As an outcome, the effectively synthesized TiO<sub>2</sub> NPs in this study were given distinction for the blue shift value of about 0.4 eV, which was associated to the phase structures, crystal size, crystallinity, and quantum size effects [30].

The current-voltage (I–V) measurement for the TiO<sub>2</sub>NPs/Si heterojunction photodetector was shown in Figure 4. It was noticed that the junction has good rectification and also noticed that the transport features were dominated via diffusion or recombination within the junction at low voltage, while the space charge limited impact became the main transport mechanism at higher bias. The value of turn-off voltage was 3.2 V. This high value was related to the high value of resistivity of TiO<sub>2</sub> film. The leakage currents in the reverse direction are low and voltage-independent and no breakdown was shown in the heterojunction for bias voltage <8 V. By using the semi-log I–V characteristic for the forward bias and the equation:  $n = (q/KT) (\Delta V / \ln(I/I_s))$ , where  $q$  is the charge of an electron,  $T$  is the temperature,  $k$  is a Boltzmann constant, and  $I_s$  is the saturation current, the ideality factor was valued and found to be 1.2, which demonstrates that the heterojunction offers the best junction assets.

Figure 5 presents the responsivity of the TiO<sub>2</sub>NPs/Si photodetector measured at 2 volt bias. As shown, a quick rise in spectral responsivity (R) was illustrated at wavelength range (210–310) nm. The maximum value was 0.71 A/W @ 310 nm owing to absorption edge of TiO<sub>2</sub> nanomaterial [31–33] film, and the additional response peak was observed in the range of 790–860 nm, related to an absorption of the substrate. Therefore, it's a good device for utilization in UV detection. Furthermore, the quantum efficiency ( $\eta$ ) for TiO<sub>2</sub>NPs/Si detectors is demarcated as the ratio of the number of produced electrons to the number of incident photons and it's determined using the formula:  $\eta = 1240R_\lambda/\lambda (nm)$ , which was found to be 2.84 at 310 nm. Owing to the broadening of the depletion width brought on by raising the reverse bias, the value is greater than unity. This finding suggests that at this reverse, the photodetector is completely exhausted, leading to effective carrier collection from photogenerated light. In addition, by absorbing photons and producing the photomultiplication effect, the

TABLE 1: XRD data for TiO<sub>2</sub> nanostructure.

$2\theta$ (degree)	Grain size (nm)	Orientation (hkl)
25.2	8	101
36.4	28	103
38.9	17	112

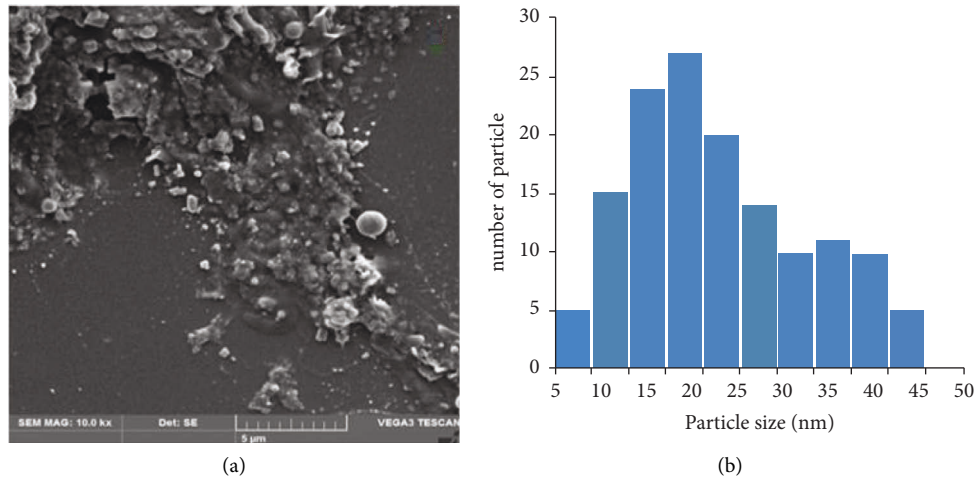


FIGURE 2: (a) SEM image of TiO<sub>2</sub>NPs and (b) size distribution.

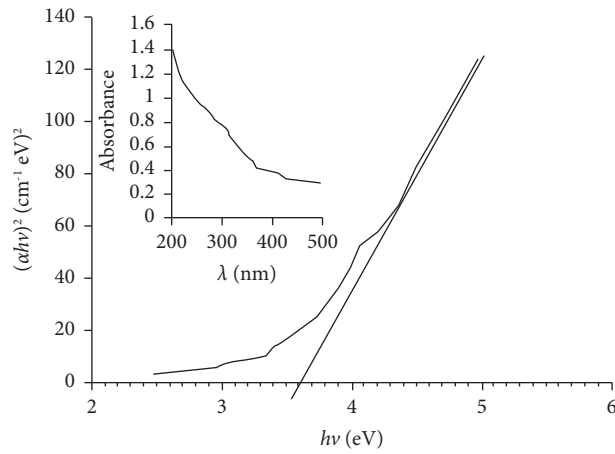


FIGURE 3: The relation between  $(\alpha hv)^2$  and  $h\nu$  of TiO<sub>2</sub> NP.

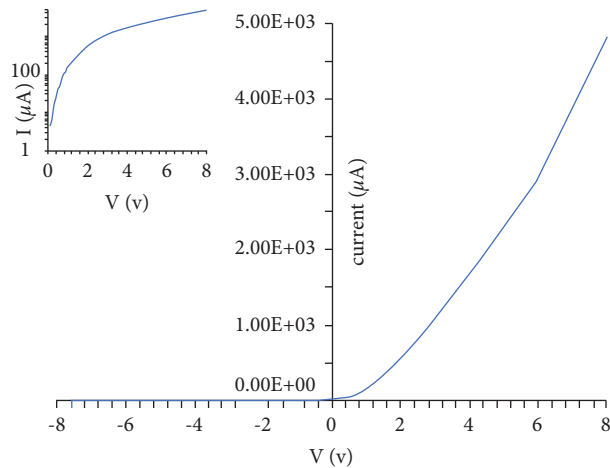


FIGURE 4:  $I_{\text{dark}}-V$  features of the TiO<sub>2</sub>NPs photodetector. In the insert figure, Semi-log  $I_f-V$  scheme.

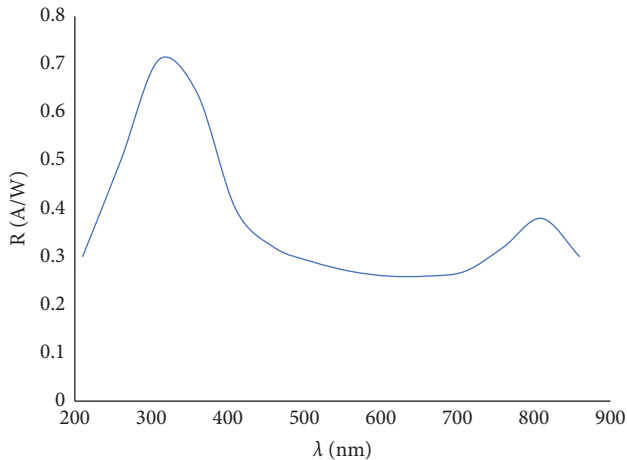


FIGURE 5: Responsivity of TiO<sub>2</sub>NPs/Si photodetector.

supplied bias dramatically raises quantum efficiency by encouraging charge injections and creating free carriers.

#### 4. Conclusion

We have a good synthesis of TiO<sub>2</sub>NPs based UV photodetector using simple pulsed Nd-YAG laser ablation of Ti metal in water. XRD results show the formation of anatase TiO<sub>2</sub>. Spherical-like shapes and sizing changes from 5 nm to 50 nm were investigated from SEM. The bandgap was 3.6 eV which was determined from the Tauc chart. The IV characteristic of the TiO<sub>2</sub>NPs/Si heterojunction showed good rectifying behavior, with the maximum responsivity of approximately 0.71 A/W at 310 nm, this method is extremely promising, simple, and low-cost for fabricating photodetectors.

#### Data Availability

The data used to support the findings of this study are included within the article.

#### Conflicts of Interest

The authors declare that there are no conflicts of interest.

#### Authors' Contributions

All authors contributed equally to this study.

#### Acknowledgments

The authors are thankful to the University of Technology, Baghdad, Iraq for support.

#### References

- [1] P. Saravanan, M. Ganapathy, A. Charles, S. Tamilselvan, R. Jeyasekaran, and M. Vimalan, "Electrical properties of green synthesized TiO<sub>2</sub> nanoparticles," *Advances in Applied Science Research*, vol. 7, no. 3, pp. 158–168, 2016.
- [2] X. Yu, X. Zou, J. Cheng et al., "Investigation on low-temperature annealing process of solution-processed TiO<sub>2</sub> electron transport layer for flexible perovskite solar cell," *Materials*, vol. 13, no. 5, Article ID 1031, 2020.
- [3] L. Wang, W. Yang, H. Chong et al., "Efficient ultraviolet photodetectors based on TiO<sub>2</sub> nanotube arrays with tailored structures," *RSC Advances*, vol. 5, no. 65, pp. 52388–52394, 2015.
- [4] K. S. Khashan, "Optoelectronic properties of ZnO nanoparticles deposition on porous silicon," *International Journal of Modern Physics B*, vol. 25, no. 02, pp. 277–282, 2011.
- [5] K. S. Khashan, A. I. Hassan, and A. J. Addie, "Characterization of CuO thin films deposition on porous silicon by spray pyrolysis," *Surface Review and Letters*, vol. 23, no. 05, Article ID 1650044, 2016.
- [6] F. A. Fadhil, B. A. Hasoon, N. N. Hussein, and K. S. Khashan, "Preparation and characterization of CuO NPs via laser ablation under electric field and study their antibacterial activity," *AIP Conference Proceedings*, vol. 2045, no. 1, Article ID 020002, 2018.
- [7] G. Govindasamy, P. Murugasen, and S. Sagadevan, "Investigations on the synthesis, optical and electrical properties of TiO<sub>2</sub> thin films by chemical bath deposition (CBD) method," *Materials Research*, vol. 19, no. 2, pp. 413–419, 2016.
- [8] S. Shadmehr, S. M. Mahdavi, N. Taghavinia, and A. Azarian, "Growth of TiO<sub>2</sub> nanoparticles by pulsed laser ablation (PLA) in liquid media and study of photocatalytic properties," *International Journal of Modern Physics B*, vol. 22, no. 18n19, pp. 3193–3200, 2008.
- [9] F. Barreca, N. Acacia, E. Barletta, D. Spadaro, G. Currò, and F. Neri, "Small size TiO<sub>2</sub> nanoparticles prepared by laser ablation in water," *Applied Surface Science*, vol. 256, no. 21, pp. 6408–6412, 2010.
- [10] E. Kumi-Barimah, R. Penhale-Jones, A. Salimian, H. Upadhyaya, A. Hasnath, and G. Jose, "Phase evolution, morphological, optical and electrical properties of femto-second pulsed laser deposited TiO<sub>2</sub> thin films," *Scientific Reports*, vol. 10, no. 1, Article ID 10144, 2020.
- [11] S. Sagadevan, "Synthesis and electrical properties of TiO<sub>2</sub> nanoparticles using a wet chemical technique," *American Journal of Nanoscience and Nanotechnology*, vol. 1, no. 1, pp. 27–30, 2013.
- [12] A. Singh, J. Vihinen, E. Frankberg, L. Hyvärinen, M. Honkanen, and E. Levänen, "Pulsed laser ablation-induced green synthesis of TiO<sub>2</sub> nanoparticles and application of novel small angle X-ray scattering technique for nanoparticle size and size distribution analysis," *Nanoscale Research Letters*, vol. 11, no. 1, p. 447, 2016.
- [13] R. Nirmala, J. W. Jeong, R. Navamathavan, and H. Y. Kim, "Synthesis and electrical properties of TiO<sub>2</sub> nanoparticles embedded in polyamide-6 nanofibers via electrospinning," *Nano-Micro Letters*, vol. 3, no. 1, pp. 56–61, 2011.
- [14] S. M. Kumbhar, S. S. Shevate, A. R. Patil, S. K. Shaikh, and K. Y. Rajpure, "Dip coated TiO<sub>2</sub> based metal-semiconductor-metal ultraviolet photodetector for UV A monitoring," *Superlattices and Microstructures*, vol. 141, Article ID 106490, 2020.
- [15] D. Solís, E. Viguera-Santiago, S. Hernández-López, A. Gómez-Cortés, M. Aguilar-Franco, and M. A. Camacho-López, "Textural, structural and electrical properties of TiO<sub>2</sub> nanoparticles using Brij 35 and P123 as surfactants," *Science and Technology of Advanced Materials*, vol. 9, no. 2, Article ID 025003, 2008.

- [16] A.-C. Lee, R.-H. Lin, C.-Y. Yang, M.-H. Lin, and W.-Y. Wang, "Preparations and characterization of novel photocatalysts with mesoporous titanium dioxide (TiO<sub>2</sub>) via a sol-gel method," *Materials Chemistry and Physics*, vol. 109, no. 2-3, pp. 275–280, 2008.
- [17] S. S. Pradhan, S. K. Pradhan, V. Bhavanasi et al., "Low temperature stabilized rutile phase TiO<sub>2</sub> films grown by sputtering," *Thin Solid Films*, vol. 520, no. 6, pp. 1809–1813, 2012.
- [18] A. Moses Ezhil Raj, V. Agnes, V. Bena Jothy, and C. Sanjeeviraja, "Low temperature TiO<sub>2</sub> rutile phase thin film synthesis by chemical spray pyrolysis (CSP) of titanyl acetylacetonate," *Materials Science in Semiconductor Processing*, vol. 13, no. 5-6, pp. 389–394, 2010.
- [19] K. S. Khashan and S. F. Abbas, "Characterization of InN nanoparticles prepared by laser as photodetector," *International Journal of Modern Physics B*, vol. 30, no. 14, Article ID 1650080, 2016.
- [20] K. S. Khashan, G. M. Sulaiman, R. Mahdi, and A. kadhim, "The effect of laser energy on the properties of carbon nanotube-iron oxide nanoparticles composite prepared via pulsed laser ablation in liquid," *Materials Research Express*, vol. 5, no. 10, Article ID 105004, 2018.
- [21] K. S. Khashan and F. Mahdi, "Synthesis of ZnO:Mg nanocomposite by pulsed laser ablation in liquid," *Surface Review and Letters*, vol. 24, no. 07, Article ID 1750101, 2017.
- [22] A. A. Hadi, B. A. Badr, R. O. Mahdi, and K. S. Khashan, "Rapid laser fabrication of Nickel oxide nanoparticles for UV detector," *Optik*, vol. 219, Article ID 165019, 2020.
- [23] K. S. Khashan and M. H. Mohsin, "Synthesis of polyynes by laser ablation of graphite in ethanol," *Iraqi Journal of Physics*, vol. 11, no. 21, pp. 37–47, 2019.
- [24] R. Hameed, K. S. Khashan, and G. M. Sulaiman, "Preparation and characterization of graphene sheet prepared by laser ablation in liquid," *Materials Today Proceedings*, vol. 20, pp. 535–539, 2020.
- [25] A. H. Hamad, K. S. Khashan, and A. A. Hadi, *Laser Ablation in Different Environments and Generation of Nanoparticles, Applications of Laser Ablation - Thin Film Deposition, Nanomaterial Synthesis and Surface Modification*, IntechOpen, 2016.
- [26] J. A. Saimon, S. N. Madhat, K. S. Khashan, and A. I. Hassan, "Characterization of CdZnO/Si heterojunction photodiode prepared by pulsed laser deposition," *International Journal of Modern Physics B*, vol. 32, no. 31, Article ID 1850341, 2018.
- [27] K. S. Khashan, J. M. Taha, and S. F. Abbas, "Fabrication and properties of InN NPs/Si as a photodetector," *Energy Procedia*, vol. 119, pp. 656–661, 2017.
- [28] K. S. Khashan, A. Hadi, M. Mahdi, and M. K. Hamid, "Nanosecond pulse laser preparation of InZnO (IZO) nanoparticles NPs for high-performance photodetector," *Applied Physics A*, vol. 125, no. 1, p. 51, 2019.
- [29] K. S. Khashan, R. A. Ismail, and R. O. Mahdi, "Synthesis of SiC nanoparticles by SHG 532 nm Nd:YAG laser ablation of silicon in ethanol," *Applied Physics A*, vol. 124, no. 6, Article ID 443, 2018.
- [30] S. K. M. Maarof, S. Abdullah, and M. Rusop Mahmood, "Structural, optical and electrical properties of titanium dioxide thin films with different molarity," *Advanced Materials Research*, vol. 667, pp. 58–62, 2013.
- [31] S. M. Nejad, S. G. Samani, and E. Rahimi, "Characterization of responsivity and quantum efficiency of TiO<sub>2</sub>-based photodetectors doped with Ag nanoparticles," in *Proceedings of the 2010 2nd International Conference on Mechanical and Electronics Engineering (ICMEE 2010)*, vol. 2, Article ID 394, Kyoto, 2010.
- [32] S. Li, T. Deng, Y. Zhang et al., "Solar-blind ultraviolet detection based on TiO<sub>2</sub> nanoparticles decorated graphene field-effect transistors," *Nanophotonics*, vol. 8, no. 5, pp. 899–908, 2019.
- [33] S.-J. Chang, T.-Y. Tsai, Z.-Y. Jiao et al., "A TiO<sub>2</sub> nanowire MIS photodetector with polymer insulator," *IEEE Electron Device Letters*, vol. 33, no. 11, pp. 1577–1579, 2012.